인터리브 부스트 컨버터용 결합형 디커플드 인덕터

파예즈 샴로즈, 무니르 무하마드 우마이르, 모하메드 아테프 타우픽, 아쉬라프 아메드, 박종후
숭실대학교 전기공학부

Integrated Decoupled Inductors for Interleaved Boost Converters

Shamroze Fayyaz, Muhammad Umair Munir, Mohamed Atef Tawfik, Ashraf Ahmed, Joung-Hu Park
Department of Electrical Engineering, Soongsil University

ABSTRACT

This paper proposes a novel concept for an integrated decoupled inductor. The proposed magnetic device features two coils, wound on a single magnetic core, arranged perpendicularly in three-dimensional space. This specific configuration ensures zero magnetic coupling between the coils, effectively transforming the integrated magnetic device into two independent inductors. The design holds promise for various DC-DC converter applications, potentially leading to advantages like cost reduction, decreased size and weight and enhanced compactness. This paper provides a comprehensive analysis of the proposed magnetic device through detailed Finite Element Method (FEM) simulations, elucidating its electromagnetic performance.

1 Introduction

The power electronics industry is in a constant pursuit of greater efficiency, reduced costs, and more compact designs. Considerable resources are invested in developing enhanced, cost-effective devices, efficient topologies, and effective control strategies [1]- [2]. The modern demands of the power electronics sector necessitate the utilization of various types of converters and inverters in diverse forms. Consequently, a wide array of topologies is continuously emerging to address varying power requirements and applications [3]. Moreover, the utilization of ISM band frequencies has enabled researchers and engineers to create smaller and more compact devices suitable for integration into existing topologies [4].

DC-DC converters are among the most prevalent and widely used converter topologies. Their applications span a broad spectrum within the industry, ranging from the integration of renewable energy sources to powering electric vehicle (EV) systems. They are also integral to various systems in medical devices and military applications [5]. With the escalating demand for load power, single DC-DC converter topologies are often interleaved to meet higher power requirements. This interleaving approach not only increases efficiency but also reduces device current ratings and minimizes current ripple [6].

One of the simplest interleaved DC-DC converter topologies is the interleaved boost converter, as illustrated in Fig. 1. Conventional DC-DC converters face challenges such as high voltage and current stress across switches and substantial current flow through the inductor. Interleaved DC-DC converters primarily address these issues by incorporating additional inductors and switches [7].

However, it's worth noting that interleaving DC-DC converters with additional inductors leads to a significant increase in volume, weight, and overall cost of the device when compared to the conventional single boost converter topology. Furthermore, as global economic growth drives increased demand for base metals and rare earth metals used in fabricating magnetic cores [8], there's a growing imperative to reduce the size of magnetic components in interleaved converters. This reduction is crucial for maintaining cost-effectiveness and sustainability in this dynamic industry.

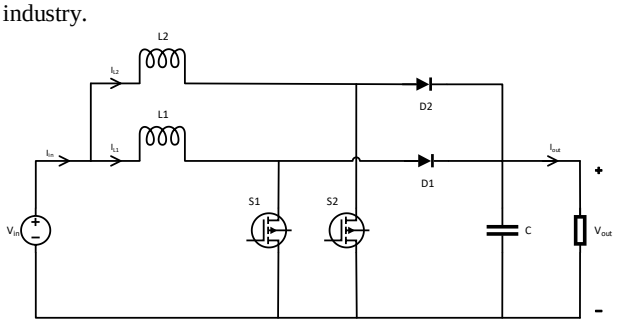

Fig. 1. Interleaved Boost Converter

Numerous design methodologies and configurations have been put forth to enhance the performance of integrated magnetic devices. One of these methods is air-gap optimization, to reduce losses in integrated coupled inductors [9]. However, it's important to note that many of these methods rely on the magnetic coupling between the inductors. This makes the design process for coupled inductors more intricate, necessitating sophisticated inductor core designs and, consequently, limiting the applicability of these devices across various fields [10]. On the other hand, when decoupled inductors are employed between interleaving phases, although it may lead to an increase in inductor current ripple, it results in a reduction in the overall output current ripple as each inductor handles only a portion of the output current [11].

This paper presents an integrated magnetic device featuring two coils wound orthogonally in space, both sharing the same cylindrical magnetic core. The careful alignment of these coils ensures zero magnetic coupling between them. The interaction of magnetic flux is thoroughly analyzed using Finite Element Method (FEM) analysis. This innovative approach simplifies the design of integrated magnetic devices, addressing issues related to magnetic coupling and offering a more versatile solution for a range of applications.

2 Proposed Integrated Inductive Device

2.1 Integrated Inductor

The proposed device consists of two coils which are wound around a single cylindrical magnetic core, spatially orthogonal to each other. Faraday's law of induction, as shown in (1) [12], states

that the induced emf, ε, in a conductor is greatest when both the magnetic flux density vector, B and the area vector, dA are in the same direction (θ = 0°) and zero if they are perpendicular to each other (θ = 90°).

$$\varepsilon = -\frac{d\phi_B}{dt} = -\frac{d}{dt}\iint \boldsymbol{B} \,.\, \boldsymbol{dA} = -\frac{d}{dt}\iint B cos\theta dA \qquad (1)$$

The windings of the proposed device were not only placed spatially orthogonal to each other, but also placed at the center of the core with respect to the winding axes to further minimize the interaction between the two coils. The spatial arrangement of the two coils around the magnetic core is shown in Fig. 2.

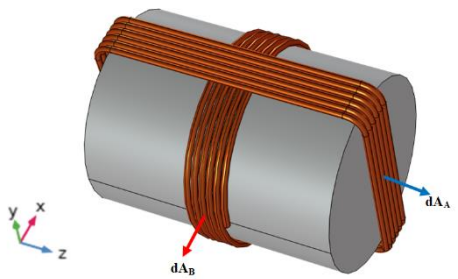

Fig. 2. Coil Orientation in the Cartesian coordinate system

2.2 Tri-axial Geometric Profiling

Consider a cylindrical magnetic core with a radius, r_o and length, l_c situated within the XYZ Cartesian coordinate system. This core houses two windings, namely winding A and winding B, which are wound orthogonal to each other on the core. Winding A lies flat on the XY plane, with its associated area vector, dA_A oriented in the direction of the Z-axis. On the other hand, winding B is positioned on the YZ plane, and its area vector, dA_B points along the X-axis.

Due to the specific orientation of these windings, each contributes to the generation of magnetic flux in two of the three Cartesian planes. Winding A produces magnetic flux in the XZ and YZ planes. Notably, the magnetic flux in the YZ plane is orthogonal to the area vector of winding B. Consequently, following Faraday's law, this magnetic flux does not affect winding B. As for the flux in the XZ plane produced by winding A, it consists of both X and Z components. Therefore, the X component of this flux is the only component that influences winding B, given its parallel alignment with the area vector of winding B.

Similarly, winding B generates magnetic flux in the XZ and XY planes. The magnetic flux in the XY plane generated by winding B is always perpendicular to the area vector of winding A, thus having no impact on winding A. The Z component of the flux in the XZ plane aligns with the area vector of winding A and influences winding A.

Each winding primarily contributes to the magnetic flux aligned with its respective area vector. Considering the spatial distribution of magnetic flux lines, the lines passing through both the horizontal and vertical centers of the core do not have an effective component that influences the other winding. As one moves away from the core's center, the corresponding effective flux component becomes increasingly significant in magnitude. However, it is crucial to emphasize that this component does not intersect the area enclosed by the winding, thereby exerting no influence on the winding itself.

3 Simulation Results

To test the hypotheses and verify the geometric analysis, two coils wound around a cylindrical magnetic core were simulated in COMSOL Multiphysics as shown in Fig. 2. The radius and length of the cylindrical magnetic core is 7.5mm and 20mm, respectively. The coils are made up of copper conductor of 0.25mm radius with 6 turns each. The coils are excited using two, external synchronized, in-phase, equal current sources. The entirety of the geometry is submerged inside a cubical air domain with the surfaces of the cube considered to be infinite.

3.1 Tri-planar Magnetic Flux Lines

When each coil is excited individually, the magnetic flux lines are formed exactly as explained earlier in section 2.2. Simulation results confirm that during dual excitation of the coils, the only plane of interaction for the magnetic flux lines from the two coils is the XZ plane as shown in Fig. 3(a). The circular path of the magnetic flux lines leads to addition of the magnetic flux lines in the second and the fourth quadrant while the magnetic flux is cancelled out in the first and the third quadrant. This leads the resultant magnetic flux to follow a path from the corner of the second quadrant leading to the corner of the fourth quadrant.

The interaction between two magnet fields or the timely change of external magnetic flux through a coil is usually considered to lead to coupling. Although the magnetic flux generated by the coils interact with each other inside the coil in three dimensions, the coupling between the coils stays zero.

The magnetic flux lines in the three planes of the Cartesian coordinate system can be seen in Fig. 3(b). The figure shows the second quadrant of the core during dual excitations of the coils. The magnetic flux lines circulating in the YZ and the XY planes are generated only by winding A and winding B, respectively.

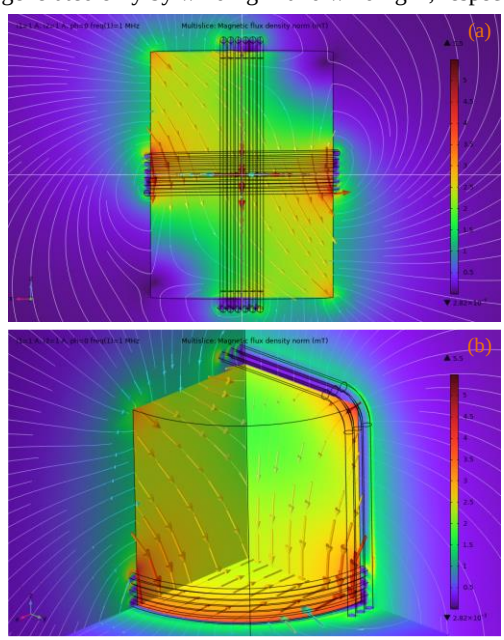

Fig. 3. FEM simulated magnetic flux density; (a) XZ plane of interaction, (b) Tri-planar Magnetic Flux Lines

3.2 Open Circuit/Short Circuit Test

The open and short circuit tests are valuable testing methodologies for determining the parameters of an inductive device, such as coupled inductors or transformers, which includes assessing the magnetic coupling between the coils.

To quantitatively determine the coupling between the two coils of the magnetic device, open and short circuit tests were conducted using COMSOL Multiphysics and 4194A Impedance Analyzer. Equation (2) is used to calculate the magnetic coupling coefficient, denoted as 'k,' between the coils. In this equation, 'L_{oc}' stands for the open circuit inductance, and 'L_{sc}' stands for short circuit inductance.

$$k = \sqrt{1 - \frac{L_{sc}}{L_{oc}}} \tag{2}$$

Both simulation and hardware results are in agreement, indicating that the magnetic coupling between the coils is less than 0.01. Ideally, the coupling between the coils should be zero. However, the slight coupling observed is primarily attributed to electrostatic interactions rather than magnetic interactions.

4 Discussion

The results indicate that the resultant magnetic flux inside the magnetic core is canceled out in some regions while being added in others, depending on the direction of the current. This suggests that, under certain conditions, the proposed magnetic device can be exploited as a variable inductor, with its inductance controlled electrically rather than mechanically.

The geometry of the proposed device and the alignment of the coils is similar to the arrangement of coils in a parametric transformer [13]. Therefore, the device can also be considered as another implementation of a parametric device, with power transfer occurring through the specific and controlled interaction of the two magnetic flux lines.

The proposed device can be enhanced by incorporating an additional coil in the third Cartesian plane, achieving magnetic decoupling and orthogonal alignment among all three coils. Such a device can serve as three independent inductors with only a single magnetic core.

COMSOL Multiphysics simulations reveal an interesting phenomenon: while there is no magnetic coupling between the coils of the magnetic device due to their orthogonal spatial alignment, there is, in fact, magnetic interaction occurring within the magnetic core geometry. Within a specific spatial point located inside the core, the effective magnetic field intensity results from the vector summation of the two magnetic field intensities generated by the two coils. This observation has led to a hypothesis: when dual excitation conditions are applied to a core with two coils, the core may saturate at a lower magnetic field intensity value, given that magnetic saturation in the core is a function of the magnetic flux density within the core geometry.

5 Conclusion

In this paper, an innovative integrated magnetic device is proposed featuring two coils wound on a single magnetic core. Despite sharing the same magnetic core, the unique alignment of the coils ensures the absence of magnetic coupling between them, effectively transforming the coils into two independent inductors. Finite Element Method (FEM) results and a geometric profile of the magnetic flux lines are provided to gain a comprehensive understanding of the magnetic flux behavior within the core. Open circuit and short circuit tests are performed to quantitatively determine the level of coupling between the coils. The tests reveal that the magnetic coupling between the coils is remarkably low, measuring less than 0.01. This low coupling coefficient emphasizes the potential of this innovative device to significantly reduce the size and cost of magnetic devices used in converters. Initial research has unveiled that, despite the absence of magnetic coupling between the two coils, the effective magnetic field intensity within the core results from the vector sum of the two magnetic field intensities generated by the two coils. Subsequent research endeavors will aim to delve into this phenomenon, investigating the impact of coil excitations of the two orthogonally aligned coils on the saturation point of the core.

References

[1] M. S. Irfan, A. M. Tawfik, A. AHmed and J.-H. Park, "Analysis and design of flux cancellation power-decoupling method for electrolytic-capacitorless three-phase cascaded multilevel inverters," *Journal of Power Electronics*, vol. 21, pp. 321-341, 2021.

[2] M. A. Tawfik, M. Ehab, A. Ahmed and J.-H. Park, "Single-Stage Isolated DC/AC Converter With Continuous Dynamic Model and Controller Design," *IEEE Transactions on Industrial Electronics*, vol. 70, no. 6, pp. 5971-5981, 2023.

[3] J. D. van Wyk and F. C. Lee, "On a Future for Power Electronics," *IEEE Journal of Emerging and Selected Topics in Power Electronics*, vol. 1, no. 2, pp. 59-72, 2013.

[4] M. Ehab, M. A. Tawfik, M. U. Munir, A. Ahmed and J.-H. Park, "ISM-Band Frequency Transformer Modeling for Isolated High-Power Conversions," *IEEE Transactions on Instrumentation and Measurement*, vol. 72, pp. 1-11, 2023.

[5] M. D. Rahman, M. Nazaf Rabbi and G. Sarowar, "Development of DC-DC Converters – A Review," in *2021 International Conference on Computational Performance Evaluation (ComPE)*, Shillong, 2021, pp. 341-347.

[6] M. N. Syah, E. Firmansyah and D. R. Utomo, "Interleaved Bidirectional DC-DC Converter Operation Strategies and Problem Challenges: An Overview," in *2022 IEEE International Conference in Power Engineering Application (ICPEA)*, Malaysia, IEEE, 2022, pp. 1-6.

[7] S. H R, S. H S and R. K C, "Comparative Analysis of Different Interleaved DC-DC Converters," in *2022 International Conference on Computer Communication and Informatics (ICCCI)*, Coimbatore, IEEE, 2022, pp. 1-6.

[8] L. Meyer and B. Bras, "Rare earth metal recycling," in *Proceedings of the 2011 IEEE International Symposium on Sustainable Systems and Technology*, Chicago, 2011, pp. 1-6.

[9] Y. Liu, H. Wu, G. Ji, S. Ni, Y. Zhang, J. Chen and Y. Xing, "Optimized Air-Gap Configuration for An Integrated Coupled Inductor with Lower Height and Reduced Core/Winding Losses," *IEEE Transactions on Industry Applications*, pp. 1-10, 2023.

[10] M. Hagemeyer, F. Schafmeister and J. Böcker, "Coupled Inductor Design for Interleaved High-Current DC-DC Converters," in *2018 21st International Conference on Electrical Machines and Systems (ICEMS)*, Jeju, IEEE, 2018, pp. 2316-2321.

[11] S. Lu, M. Mu, Y. Jiao, F. C. Lee and Z. Zhao, "Coupled Inductors in Interleaved Multiphase Three-Level DC–DC Converter for High-Power Applications," *IEEE Transactions on Power Electronics*, vol. 31, no. 1, pp. 120-134, 2016.

[12] P. Kinsler, "Faraday's Law and Magnetic Induction: Cause and Effect, Experiment and Theory," *Physics*, vol. 2, no. 2, pp. 150-163, 2020.

[13] E. S. Tez, "The Parametric Transformer," 1977.